Thin Film Deposition Using Spray Pyrolysis

Journal Article

Author(s):
Perednis, Dainius; Gauckler, Ludwig J.

Publication date:
2005-03

Permanent link:
https://doi.org/10.3929/ethz-b-000033131

Originally published in:
Journal of electroceramics 14(2), https://doi.org/10.1007/s10832-005-0870-x

Journal of Electroceramics, 14, 103–111, 2005

Thin Film Deposition Using Spray Pyrolysis

DAINIUS PEREDNIS & LUDWIG J. GAUCKLER
Nonmetallic Inorganic Materials, Department of Materials, Swiss Federal Institute of Technology, Wolfgang-Pauli-Str. 10, CH-8093 Zurich, Switzerland

Submitted August 29, 2003; Revised August 2, 2004; Accepted August 2, 2004

Abstract. Spray pyrolysis has been applied to deposit a wide variety of thin films. These films were used in various devices such as solar cells, sensors, and solid oxide fuel cells. It is observed that often the properties of deposited thin films depend on the preparation conditions. An extensive review of the effects of spray parameters on film quality is given to demonstrate the importance of the process of optimization. The substrate surface temperature is the most critical parameter as it influences film roughness, cracking, crystallinity, etc. Processes involved in the spray pyrolysis technique are discussed in this review as well.

Keywords: spray pyrolysis, thin films, properties of deposited films

1. Introduction

The application of thin films in modern technology is widespread. The methods employed for thin-film deposition can be divided into two groups based on the nature of the deposition process viz., physical or chemical. The physical methods include physical vapour deposition (PVD), laser ablation, molecular beam epitaxy, and sputtering. The chemical methods comprise gas-phase deposition methods and solution techniques (Fig. 1). The gas-phase methods are chemical vapour deposition (CVD) [1, 2] and atomic layer epitaxy (ALE) [3], while spray pyrolysis [4], sol-gel [5], spin- [6] and dip-coating [7] methods employ precursor solutions.

Spray pyrolysis is a processing technique being considered in research to prepare thin and thick films, ceramic coatings, and powders. Unlike many other film deposition techniques, spray pyrolysis represents a very simple and relatively cost-effective processing method (especially with regard to equipment costs). It offers an extremely easy technique for preparing films of any composition. Spray pyrolysis does not require high-quality substrates or chemicals. The method has been employed for the deposition of dense films, porous films, and for powder production. Even multilayered films can be easily prepared using this versatile technique. Spray pyrolysis has been used for several decades in the glass industry [8] and in solar cell production [9].

Typical spray pyrolysis equipment consists of an atomizer, precursor solution, substrate heater, and temperature controller. The following atomizers are usually used in spray pyrolysis technique: air blast (the liquid is exposed to a stream of air) [10], ultrasonic (ultrasonic frequencies produce the short wavelengths necessary for fine atomization) [11] and electrostatic (the liquid is exposed to a high electric field) [12].

Various reviews concerning spray pyrolysis techniques have been published. Mooney and Radding have reviewed the spray pyrolysis method, properties of the deposited films in relation to the conditions, specific films (particularly CdS), and device application [13]. Tomar and Garcia have discussed the preparation and the properties of sprayed films as well as their application in solar cells, anti-reflection coatings, and gas sensors [14]. Albin and Risbud presented a review of the equipment, processing parameters, and optoelectronic materials deposited by the spray pyrolysis technique [15]. Pamplin has published a review of spraying solar cell materials as well as a bibliography of references on the spray pyrolysis technique [16]. Recently, thin metal oxide and chalcogenide films deposited by spray pyrolysis and different atomization techniques were reviewed by Patil [17]. Bohac and Gauckler have

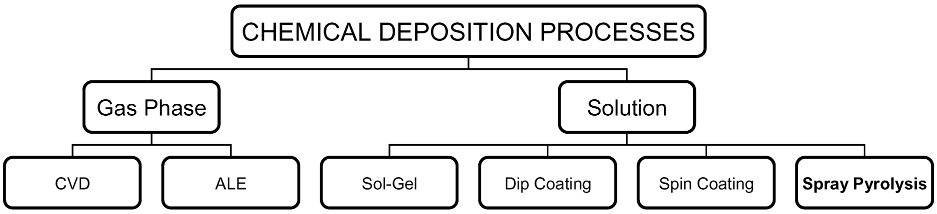

Fig. 1. Chemical thin film deposition methods.

discussed the mechanism of chemical spray deposition and presented some examples of sprayed YSZ films [18].

Film deposition using spray pyrolysis will be discussed in this review. The influence of deposition temperature and precursor solution on film structure and properties will be illustrated with some examples. Models for thin-film deposition by spray pyrolysis will also be reviewed.

2. Influence of Deposition Parameters on Thin Film Properties

Thin-film deposition, using the spray pyrolysis technique, involves spraying a metal salt solution onto a heated substrate (Fig. 2). Droplets impact on the substrate surface, spread into a disk shaped structure, and undergo thermal decomposition. The shape and size of the disk depends on the momentum and volume of the droplet, as well as the substrate temperature. Consequently, the film is usually composed of overlapping disks of metal salt being converted into oxides on the heated substrate.

This section deals with the influence of the main spray pyrolysis parameters on structure and properties of the deposited films.

2.1. *Influence of Temperature*

Spray pyrolysis involves many processes occurring either simultaneously or sequentially. The most important of these are aerosol generation and transport, solvent evaporation, droplet impact with consecutive spreading, and precursor decomposition. The deposition temperature is involved in all mentioned processes, except in the aerosol generation. Consequently, the substrate surface temperature is the main parameter that determines the film morphology and properties. By increasing the temperature, the film morphology can change from a cracked to a porous microstructure. In many studies the deposition temperature was reported indeed as the most important spray pyrolysis parameter.

The properties of deposited films can be varied and thus controlled by changing the deposition temperature, for instance, it influences optical and electrical

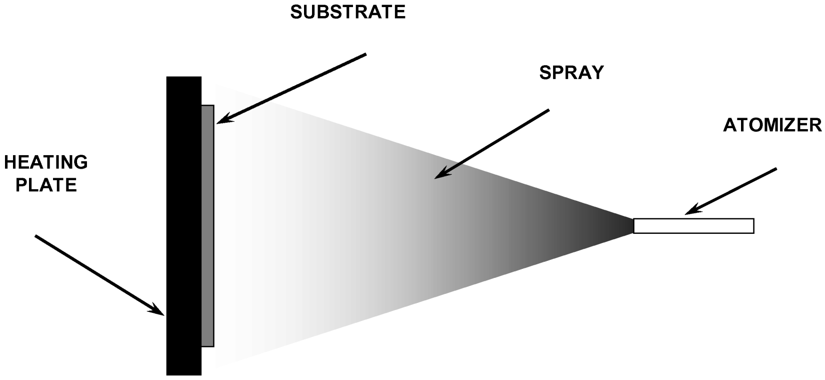

Fig. 2. Schematic diagram of spray pyrolysis equipment.

properties of zinc oxide films [19]. Films with the lowest electrical resistivity were deposited using an aqueous solution of zinc acetate at 490°C resulting in improved crystallinity, while films prepared at 420 and 490°C showed high transmission (90–95%) in the visible range. This was attributed to a decrease of the film thickness and an increase in the structural homogeneity.

The physical properties of fluorine-doped indium oxide films were investigated with respect to deposition temperature, dopant concentration, air flow rate, and film thickness [20]. It was found that the deposition temperature has a remarkable influence on the structure of the films. The extent of preferential (4 0 0) orientation increases with increasing film thickness.

Terbia-doped yttria-stabilized thin films have been deposited using electrostatic spray deposition [21]. The surface morphology was controlled by changing the deposition parameters and solution compositions. By increasing the deposition temperature, the morphology of the film was shifted from a dense to a highly porous structure.

2.2. *Influence of Precursor Solution*

The precursor solution is the second important process variable. Solvent, type of salt, concentration of salt, and additives influence the physical and chemical properties of the precursor solution. Therefore, structure and properties of a deposited film can be tailored by changing composition of precursor solution.

Chen et al. have shown that the morphology of the thin films can be changed considerably by adding additives to the precursor solutions [22]. The structure of deposited TiO_2 film was changing from a cracked to a crack-free reticular after the introduction of acetic acid into the precursor solution. The change of morphology was attributed to the modification of precursor solution chemistry.

Transparent SnO_2 electrodes were deposited by spray pyrolysis using tetra-*n*-butyltin (IV) as precursor [23]. The deposition efficiency and crystallinity of the films deposited at 340°C was improved by adding H_2O_2 to the alcoholic precursor solution. The authors proposed two explanations for this effect. One was that H_2O_2 decomposes easily on a substrate to produce an oxygen atmosphere, which promotes the oxidation of tetra-*n*-butyltin and reduces residuals within the film. The second was that H_2O_2 and tetra-*n*-butyltin form tin peroxide complexes with direct atomic bondings between tin and oxygen in the precursor solution. This kind of structure is desirable for formation of SnO_2. The second explanation is more reasonable, because in the spray pyrolysis process usually there is enough oxygen in air for the oxidation of salts.

Porous SnO_2 and SnO_2-Mn_2O_3 films have been prepared using the electrostatic spray deposition technique [24, 25]. These films were used in Taguchi type hydrogen sensors. The grain size of the porous films ranged from 1 to 10 μm. It was observed that the grain size increases with a higher concentration of the precursor in the ethanol solvent.

Caillaud et al. investigated the influence of pH of the solution on the thin film deposition and found that the growth rate depended on the pH [26]. The rate was only significant if $3.5 \leq \text{pH} \leq 4.3$. In this pH range the vaporized precursors are the zinc acetate complexes. Formation of basic salts, adsorption compounds, or precipitates slowed down the growth at higher pH. At low pH, both the amount of zinc acetate and the growth rate decrease until no more deposition occurs.

Thin SnO_2 films for gas sensors have been prepared also by spray pyrolysis using an inorganic as well as an organic precursor solution [27]. Smooth but not very uniform films were obtained using a solution of $(NH_4)_2SnCl_6$ in water. On the other hand, very uniform but relatively rough films were deposited using a solution of $(CH_3COO)_2SnCl_2$ in ethylacetate. Suitable electric properties were measured for films obtained from the organic solution. The sensitivity and rise time were found to depend on the deposition temperature and the type of precursor solution used. The best results were achieved by spraying an organic precursor solution onto a substrate at about 300°C.

In [11] the effect of glycerol in aqueous nitrate solutions on the growth of $YBa_2Cu_3O_7$ (YBCO) films was reported. The superconductor films on YSZ substrates prepared from precursor solutions with glycerol showed a sharp superconducting transition, a T_c as for bulk material (above 90 K), and a strong c-axis-oriented texture. On the other hand, the surface of the film prepared from the aqueous precursor solution was irregular, and had a lower T_c than the bulk material. Authors suggested that glycerol improves the production of fine droplets, thus improving the surface morphology of the deposited film.

It was observed that the growth rate of SnO_2 films prepared from $SnCl_4 \cdot 5H_2O$ was higher and their resistance lower in comparison with those prepared from anhydrous $SnCl_4$ [28]. The authors suggested that under identical conditions, the droplets containing $SnCl_4 \cdot 5H_2O$ require more thermal energy to form SnO_2 than those containing $SnCl_4$. Thus the water molecules seemed to influence the reaction kinetics, particularly the growth rate of the films.

The influence of process parameters on the sensitivity to humidity of SnO_2-Fe_2O_3 films has been investigated [29]. The nature of the iron salt influenced the humidity sensitivity of the samples. The films deposited from an alcohol solution containing $Fe_2(C_2O_4)_3$ exhibit higher sensitivity than from a solution containing $Fe(NH_4)(SO_4)_2$. This fact was explained by the higher porosity of the structure obtained from iron oxalate, because during the oxalate pyrolysis a lot more gaseous decomposition products are released compared to the sulphate precursors.

Kim et al. have studied the influence of additives on the properties of MgO films deposited by electrostatic spray deposition [30]. A large number of separated particles were observed on the surface of MgO films when pure tetrahydrofuran (THF) was used as a solvent. However, smooth and particle free MgO films were deposited when 1-butyl alcohol or 1-octyl alcohol was added to THF. The authors suggest that the alcohols effectively restrain MgO nucleation resulting from the vaporization of droplets.

3. Models for Film Deposition by Spray Pyrolysis

Only very crude models about the mechanism of spray deposition and film formation have been developed up to now. There are too many processes that occur either sequentially or simultaneously during film formation by spray pyrolysis for these to be modelled in a straightforward manner. These include precursor solution atomization, droplet transport and evaporation, spreading on the substrate, drying and decomposition of the precursor salt. Understanding these processes will help to improve film quality. Thin-film deposition using spray pyrolysis can be divided into three main steps: atomization of the precursor solution, transportation of the resultant aerosol, and decomposition of the precursor on the substrate.

3.1. Atomization of Precursor Solution

Atomization of liquids has been investigated for many years. The key is to understand the basic atomization process of the atomization device in use. In particular, it is important to know which type of atomizer is best suited for which application and how the performance of the atomizer is affected by variations in liquid properties and operating conditions. Air blast, ultrasonic, and electrostatic atomizers are normally used in spray pyrolysis techniques.

Numerous reports were published on the mechanism of liquid atomization. Rizkalla and Lefebvre examined the influence of liquid properties on air blast atomizer spray characteristics [31]. Lampkin presented results concerning the application of the air blast atomizer in a spray pyrolysis set-up [32]. Recently, a theory of ultrasonic atomization was published [33]. Ganan-Calvo et al. have studied the electrostatic atomization of liquids and derived scaling laws for droplet size from a theoretical model of charge transport [34, 35].

Compared with other spray techniques, the electrostatic spray deposition technique has been used only recently for thin-film deposition, whereas liquid atomization by means of an electric field has been investigated for many years. Research into electrostatic spray deposition started with Rayleigh's study on the stability of an isolated charged droplet [36]. Electrostatic atomization of liquid was first reported by Zeleny [37]. Grace and Marijnissen have published a review on this type of atomization [38]. Depending on spray parameters, various spraying modes are obtained, resulting in very different droplet size distributions. Cloupeau et al. proposed a classification of these modes [39]. Cone-jet and multi-jet modes are the most important modes for spray deposition. In the cone-jet mode the liquid is distorted at the tip of the tube type nozzle into a conical shape (Taylor cone). This cone is extended at its apex by a permanent jet of very small diameter (see Fig. 3). The jet usually emits charged mono-dispersed droplets. With increasing electric field, the jet may be split, forming a multi-jet mode where the number of jets increases with applied voltage (see Fig. 4).

3.2. Aerosol Transport

In an aerosol the droplet is transported and eventually evaporates. During transportation it is important that as many droplets as possible are transported to the

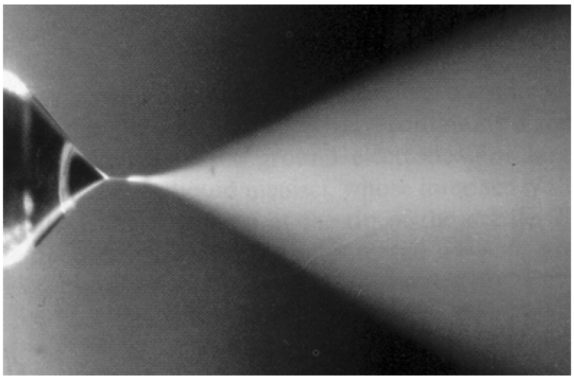

Fig. 3. Cone-jet spraying of methanol containing a small amount of hydrochloric acid [35].

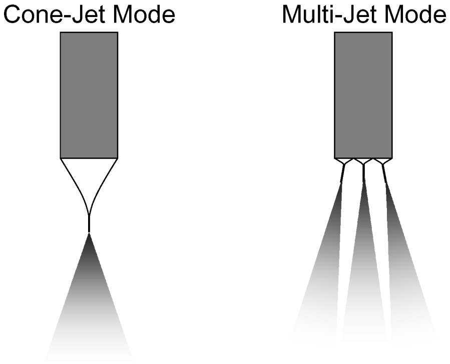

Fig. 4. Cone-jet and multi-jet modes.

substrate without forming powder or salt particles. Sears et al. investigated the mechanism of SnO_2 film growth [40]. The influence of forces which determine both the trajectory of the droplets and evaporation were examined and a film growth model was proposed. Gravitational, electric, thermophoretic and Stokes forces were taken into account. The thermophoretic force pushes the droplets away from a hot surface, because the gas molecules from the hotter side of the droplet rebound with higher kinetic energy than those from the cooler side. For example, at a surface temperature of 350°C and a thermal gradient of 500°C/cm it was calculated that the thermophoretic force is equal to the gravitational force for a droplet of 2 μm in diameter. Thermophoretic forces keep most droplets away from the surface in non-electrostatic spray process. However, most aerosols contain many droplets significantly larger than 2 μm. It follows that the authors overestimated the role of thermophoretic forces. Additionally, it was concluded that the film grows from the vapour of droplets passing very close to the hot substrate in a manner of chemical vapour deposition and droplets that strike the substrate form a powdery deposit (Fig. 5). However, the authors have not considered the spreading of droplets on the substrate, which more significantly contributes to the film growth. In the spray pyrolysis process it is desired that the most droplets strike the substrate and spread.

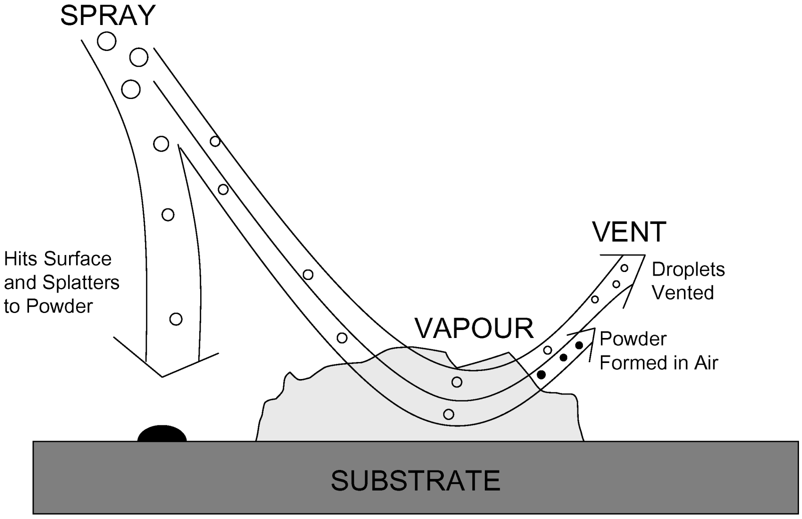

Fig. 5. Aerosol transport.

Siefert described the transport processes in corona spray pyrolysis. Here the droplets enter a corona discharge and are transported in an electric field to the substrate [41]. The following forces were taken into account: gravitational, Stokes, thermophoretic, electric, and dielectric forces. The author has calculated that only droplets, with a radius larger than 5 μm, will contribute to film formation at a substrate temperature of 430°C. This value depends on the composition of the solution, the applied voltage and the deposition temperature. The solvent is entirely vaporized in the smaller droplets that will consequently lead to powder formation. However, the authors have not considered formation of hollow particles during the transportation.

The aerosol droplets experience evaporation of the solvent during the transport to the substrate. This leads to a size reduction of the droplet and to the development of a concentration gradient within the droplet. The precursor precipitates on the surface of the droplet, when the surface concentration exceeds the solubility limit. Precipitation occurs due to rapid solvent evaporation and slow solute diffusion. This results in the formation of a porous crust and subsequently hollow particles, which are not desired because they increase the film roughness.

Yu and Liao developed a model describing the evaporation of solution droplets before the formation of a solid crust [42]. The transfer of mass, momentum, temperature outside and around the droplet as well as effects of precursor precipitation were taken into account. The interactions between droplets were ignored. Rapid increases in droplet temperatures were observed at the beginning of evaporation and at the moment when precursor precipitation on the droplet surface starts. This temperature increase was due to heat evolved as a result of precipitation. At the beginning of this process the evaporation rate very quickly reaches a maximum, then decreases until precipitation takes place. This rate accelerates again simultaneously with droplet temperature when precipitation starts. Increasing the gas temperature caused a steeper concentration gradient inside the droplet. The effects of humidity of the ambient gas were found to be insignificant. Lenggoro et al. investigated powder production by spray pyrolysis using a temperature-graded laminar flow aerosol reactor [43]. They presented calculations results for the evaporation rate and the change of the precursor concentration within the droplets. The predicted numerical simulation results were in good agreement with the experimental results. The simulations indicated that the solid particles can be formed when the reactor temperature is low and constant or distributed inhomogeneously, when the precursor solution concentration is high and when the flow rate of carrier gas is low. Undesired hollow particles are formed when the droplets are large and the droplet number concentration is low. Smaller droplets produce solid particles because the diffusion distance for the solute is shorter, leading to a more uniform concentration distribution within the droplet. Increasing the number of droplets results in a larger solvent vapour concentration in the carrier gas. Consequently, the evaporation rate decreases and precipitation is delayed. Therefore, an increase in the number of droplets decreases the probability of forming hollow particles.

Oh and Kim have studied the behaviour of an evaporating droplet in a non-isothermal field [44]. An alcoholic solution of titanium tetraethoxide was atomized by an ultrasonic nebulizer. Nitrogen was used as carrier gas. The flow and temperature profiles of the carrier gas were calculated and then the motion and evaporation of the droplets simulated numerically. Measurements of deposition efficiency and film thickness distribution were compared with calculated particle trajectories. The comparisons have shown that the deposition efficiency and the area coated increase with the amount of sprayed solution and carrier gas flow rate, but decrease with nozzle-to-substrate distance.

3.3. Decomposition of Precursor

Many processes occur simultaneously when a droplet hits the surface of the substrate: evaporation of residual solvent, spreading of the droplet, and salt decomposition. Many models exist for the decomposition of a precursor. Most of the authors suggest that only a kind of CVD process gives high quality films by spray pyrolysis.

Viguie and Spitz proposed the following processes that occur with increasing substrate temperature [45]. In the lowest temperature regime (process A) the droplet splashes onto the substrate and decomposes (Fig. 6). At higher temperatures (process B) the solvent evaporates completely during the flight of the droplet and dry precipitate hits the substrate, where decomposition occurs. At even higher temperatures (process C) the solvent also evaporates before the droplet reaches the substrate. Then the solid precipitate melts and vaporizes without decomposition and the vapour diffuses to the substrate to undergo a CVD process. At the

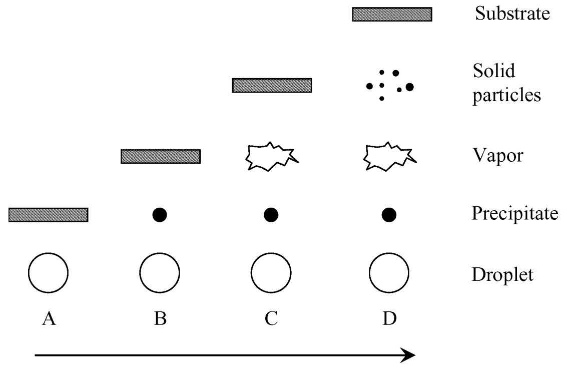

Fig. 6. Description of the deposition processes initiated with increasing substrate temperature.

highest temperatures (process D) the precursor vaporizes before it reaches the substrate, and consequently the solid particles are formed after the chemical reaction in the vapour phase. It is believed that the processes A and D lead to rough or non-adherent films. Adherent films were obtained by CVD at low temperatures (process C). However, type A or B allows formation of high quality adherent films too. Moreover, the process C can rarely occur in most spray pyrolysis depositions, because either the deposition temperature is too low for the vaporization of a precursor or the precursor salt decomposes without melting and vaporization.

Choy proposed a deposition model for the so-called electrostatic spray-assisted vapour deposition process [46]. This technique is also known as electrostatic spray deposition. The precursor solution is atomized using an electric field. Porous and amorphous CdS films were obtained below 300°C (process I). At high substrate temperatures (above 450°C) powdery films were produced due to the vaporization and decomposition of the precursor before reaching the substrate (process III). At intermediate temperatures (300–450°C), both processes may occur. The authors suggest that at the optimum temperature the solvent evaporates close to the substrate, and the precursor is volatilized near the vicinity of the substrate and adsorbed onto the surface, followed by decomposition to yield a dense film with good adhesion (process II). This would correspond again to a heterogeneous CVD reaction. It was estimated that the optimum temperature lies between 400°C and 450°C. The presence of large particles on the surface was attributed to very large droplets, which might not decompose through the CVD process route when they arrive at the substrate.

Chen et al. investigated the correlations between film morphologies and deposition parameters [12]. The films were deposited using the so-called cone-jet mode. It was concluded that the morphology of the film deposited by ESD is determined by the size of the incoming droplets, deposition temperature, the rate of droplets spreading on the substrate, and solution chemistry. The substrate temperature was indicated as the most important parameter. The concentration of the precursor solution had a minor influence on the film morphology.

Kosugi et al. has separated the Cu_2O film deposition process into four steps: (1) arrival of droplets, followed by reduction of the Cu^{2+} to elementary copper with glucose; (2) formation and condensation of copper clusters; (3) oxidation of the copper clusters to Cu_2O clusters; (4) growth and densification of Cu_2O clusters [47].

The salt decomposition plays an important role in the spray pyrolysis technique. Stryckmans et al. investigated the decomposition of magnesium acetylacetonate ($Mg(acac)_2$) and the following model was suggested [48]. After melting at 265°C, $Mg(acac)_2$ is no longer stable. The molecule splits and gives a gaseous organic fragment ($C_5H_7O_2$) and a liquid compound containing magnesium ($MgC_5H_7O_2$). The gaseous fragment is degraded into smaller molecules. The compound containing the magnesium is slowly degraded to form MgO and organic residues. Higher weight loss than theoretically predicted for the formation of MgO from $MgC_5H_7O_2$ was observed between 290 and 600°C. It indicates that the $MgC_5H_7O_2$ liquid phase is partially evaporated. Smooth films were deposited in the temperature range 350–420°C. However, some cracks were still observed.

Zirconium acetylacetonate ($Zr(acac)_4$) was often used as precursor in spray deposition of zirconia films. Little information is available in the literature about the decomposition of this salt. Ismail studied the decomposition reactions of $Zr(acac)_4$ in dry nitrogen [49]. The results showed that the $Zr(C_5H_7O_2)_4$ had completely decomposed to ZrO_2 at 800°C, through intermediates $Zr(CH_3COO)_2(C_5H_7O_2)_2$ at 190°C, $ZrO(CH_3COO)_2$ at 340°C and $ZrOCO_3$ at 450°C.

Wang et al. investigated the thermal decomposition of $Zr(acac)_4$ in air using thermo-gravimetry and infrared spectrometry [50]. Weight loss occurred in three temperature regions: at 110–187°C, 187–245°C and 245–440°C. The IR spectrum of $Zr(acac)_4$ heated at different temperatures from room temperature to 450°C indicated that all acetylacetone structures decompose completely at 310°C. The above investigations suggest that Zr(acac)$_4$ does not sublime at atmospheric pressure and the decompositions of precursor compounds are accomplished at 440°C.

Often the CVD mechanism is assumed for the formation of dense films. However, formation of films from non-volatile nitrates, low deposition temperatures, and splats observed on the film surface contradict a CVD process. Matsuzaki et al. prepared YSZ films using volatile zirconium octylate and yttrium octylate as precursors at unusually high substrate temperatures of 600–750°C [51]. Two possible reactions for the film growth were considered, namely the precursors reach the substrate surface in a liquid state and pyrolyze, or the droplets turn into vapors and form the film by the CVD process. In order to choose the growth mechanism, the yttrium content in the film was measured by fluorescent X-ray analysis. The same yttrium content in the precursor solution and in the deposited film was measured. Also no temperature dependence of the yttrium content in the film was observed. These two facts are in contradiction with a CVD mechanism. The vapour pressures of yttrium and zirconium octylates are different, and therefore different yttrium contents are expected in the film and in the solution. Since the vapour pressure changes with temperature, also a temperature dependence of the yttrium content in the film is expected. As this was not the case, they proposed a deposition mechanism without CVD character.

4. Summary

Spray pyrolysis is a versatile and effective technique to deposit metal oxide films. The quality and properties of the films depend largely on the process parameters. The most important parameter is the substrate surface temperature. The higher the substrate temperature, the rougher and more porous are the films. If the temperatures are too low the films are cracked. The deposition temperature also influences the crystallinity, texture, and other physical properties of the deposited films. The precursor solution is the other important spray parameter, which affects the morphology and the properties of the deposited films. In addition, the film morphology and properties can be drastically changed by using various additives in the precursor solution.

It is often suggested that a modified CVD process occurs close to the surface of the substrate. However many observations contradict the involvement of a model with a CVD character. Further efforts are necessary to clarify the model for film deposition.

References

1. W.A. Bryant, *J. Mater. Sci.*, **12**(7), 1285 (1977).
2. R.N. Ghoshtagore, *J. Electrochem. Soc.*, **125**(1), 110 (1978).
3. T. Suntola, *Thin Solid Films*, **216**(1), 84 (1992).
4. R.R. Chamberlin and J.S. Skarman, *J. Electrochem. Soc.*, **113**(1), 86 (1966).
5. C.J. Brinker, A.J. Hurd, G.C. Frye, K.J. Ward, and C.S. Ashley, *J. Non-Cryst. Solids*, **121**(1–3), 294 (1990).
6. C.C. Chen, M.M. Nasrallah, and H.U. Anderson, *J. Electrochem. Soc.*, **140**(12), 3555 (1993).
7. C.J. Brinker, G.C. Frye, A.J. Hurd, and C.S. Ashley, *Thin Solid Films*, **201**(1), 97 (1991).
8. J.M. Mochel, US Patent 2,564,707 (1951).
9. J.E. Hill and R.R. Chamberlin, US Patent 3,148,084 (1964).
10. A.R. Balkenende, A. Bogaerts, J.J. Scholtz, R.R.M. Tijburg, and H.X. Willems, *Philips Journal of Research*, **50**(3–4), 365 (1996).
11. S.P.S. Arya and H.E. Hintermann, *Thin Solid Films*, **193**(1–2), 841 (1990).
12. C.H. Chen, E.M. Kelder, P.J.J.M. van der Put, and J. Schoonman, *J. Mater. Chem.*, **6**(5), 765 (1996).
13. J.B. Mooney and S.B. Radding, *Annu. Rev. Mater. Sci.*, **12**, 81 (1982).
14. M.S. Tomar and F.J. Garcia, *Progress in Crystal Growth and Characterization of Materials*, **4**(3), 221 (1981).
15. D.S. Albin and S.H. Risbud, *Advanced Ceramic Materials*, **2**(3A), 243 (1987).
16. B.R. Pamplin, *Progress in Crystal Growth and Characterization of Materials*, **1**(4), 395 (1979).
17. P.S. Patil, *Mater. Chem. Phys.*, **59**(3), 185 (1999).
18. P. Bohac and L.J. Gauckler, in *Oxygen Ion and Mixed Conductors and their Technological Applications*, edited by H.L. Tuller, J. Schoonman, and I. Riess (Kluwer Academic Publishers, Dordrecht, 2000), p. 271.
19. H.H. Afify, S.A. Nasser, and S.E. Demian, *J. Mater. Sci.: Materials in Electronics*, **2**(3), 152 (1991).
20. S. Mirzapour, S.M. Rozati, M.G. Takwale, B.R. Marathe, and V.G. Bhide, *J. Mater. Sci.*, **29**(3), 700 (1994).
21. N.H.J. Stelzer and J. Schoonman, *J. Materials Synthesis and Processing*, **4**(6), 429 (1996).
22. C.H. Chen, E.M. Kelder, and J. Schoonman, *J. Eur. Ceram. Soc.*, **18**, 1439 (1998).
23. M. Okuya, S. Kaneko, K. Hiroshima, I. Yagi, and K. Murakami, *J. Eur. Ceram. Soc.*, **21**(10–11), 2099 (2001).
24. H. Gourari, M. Lumbreras, R. Van Landschoot, and J. Schoonman, *Sensors and Actuators B*, **47**(1–3), 189 (1998).
25. H. Gourari, M. Lumbreras, R. Van Landschoot, and J. Schoonman, *Sensors and Actuators B*, **58**(1–3), 365 (1999).
26. F. Caillaud, A. Smith, and J.F. Baumard, *J. Amer. Ceram. Soc.*, **76**(4), 998 (1993).
27. H. Pink, L. Treitinger, and L. Vite, *Jpn. J. Appl. Phys.*, **19**(3), 513 (1980).
28. V. Vasu and A. Subrahmanyam, *Thin Solid Films*, **193** (1–2), 973 (1990).

29. T.M. Racheva, I.D. Stambolova, and T. Donchev, *J. Mater. Sci.*, **29**(1), 281 (1994).
30. S.G. Kim, K.H. Choi, J.H. Eun, H.J. Kim, and C.S. Hwang, *Thin Solid Films*, **377**, 694 (2000).
31. A.A. Rizkalla and A.H. Lefebvre, *J. Eng. Power*, **97**(2), 173 (1975).
32. C.M. Lampkin, *Progress in Crystal Growth and Characterization of Materials*, **1**(4), 405 (1979).
33. R. Rajan and A.B. Pandit, *Ultrasonics*, **39**(4), 235 (2001).
34. A.M. Ganan-Calvo, J. Davila, and A. Barrero, *J. Aerosol Sci.*, **28**(2), 249 (1997).
35. C. Pantano, A.M. Ganan-Calvo, and A. Barrero, *J. Aerosol Sci.*, **25**(6), 1065 (1994).
36. F.R.S. Rayleigh, *Phil. Magazine*, **14**, 184 (1882).
37. J. Zeleny, *The Physical Review*, **3**(2), 69 (1914).
38. J.M. Grace and J.C.M. Marijnissen, *J. Aerosol Sci.*, **25**(6), 1005 (1994).
39. M. Cloupeau and B. Prunet-Foch, *J. Electrostatics*, **25**(2), 165 (1990).
40. W.M. Sears and M.A. Gee, *Thin Solid Films*, **165**(1), 265 (1988).
41. W. Siefert, *Thin Solid Films*, **120**(4), 267 (1984).
42. H.F. Yu and W.H. Liao, *Int. J. Heat and Mass Transfer*, **41**(8–9), 993 (1998).
43. I.W. Lenggoro, T. Hata, F. Iskandar, M.M. Lunden, and K. Okuyama, *J. Mater. Res.*, **15**(3), 733 (2000).
44. E.K. Oh and S.G. Kim, *J. Aerosol Sci.*, **27**(8), 1143 (1996).
45. J.C. Viguie and J. Spitz, *J. Electrochem. Soc.*, **122**(4), 585 (1975).
46. K.L. Choy and B. Su, *Thin Solid Films*, **388**(1–2), 9 (2001).
47. T. Kosugi and S. Kaneko, *J. Amer. Ceram. Soc.*, **81**(12), 3117 (1998).
48. O. Stryckmans, T. Segato, and P.H. Duvigneaud, *Thin Solid Films*, **283**(1–2), 17 (1996).
49. H.M. Ismail, *Powder Technology*, **85**(3), 253 (1995).
50. H.B. Wang, C.R. Xia, G.Y. Meng, and D.K. Peng, *Materials Letters*, **44**(1), 23 (2000).
51. Y. Matsuzaki, M. Hishinuma, and I. Yasuda, *Thin Solid Films*, **340**(1–2), 72 (1999).